Observational Study

Medicine®

OPEN

Effects of nonvalvular atrial fibrillation on the structure and function of mitral valves (a STROBE-compliant article)

Dan-qing Huang, MD, Cun-ying Cui, MD, Juan Zhang, MD, Yuan-yuan Liu, MD, Yun-yun Qin, MD, Lian-zhong Zhang, PhD, Lin Liu, PhD*

Abstract

The aim of this study was to explore the effects of nonvalvular atrial fibrillation (NVAF) on the structure and function of mitral valve and analyze independent risk factors of moderate to severe mitral regurgitation (MR) by quantitative measurement of mitral parameters using real-time 3-dimensional transesophageal echocardiography.

This study included 30 subjects with sinus rhythm group, and 65 patients with NVAF. The 65 patients with NVAF were divided into 35 with paroxysmal atrial fibrillation group and 30 with persistent atrial fibrillation. According to MR degree, the patients with NVAF were again divided into no or mild MR group (n = 44) and moderate to severe MR group (n = 21).

There were significant differences in anterolateral-to-posteromedial diameter (DAlPm), anterior-to-posterior diameter, 3-dimensional circumference (C3D), 2-dimensional area (A2D), mitral leaflet surface area in late systolic phase, the index of mitral valve coaptation and left atrial internal diameter (LAID) between different cardiac rhythm groups (all $P < .05$). The DAlPm, C3D, A2D, nonplanar angle (θNPA), and LAID were greater but the mitral valve coaptation index was smaller in the moderate to severe MR group than in the no or mild MR group (all $P < .05$). Logistic regression analysis indicated that DAlPm and LAID were independent risk factors of moderate to severe MR in the patients with NVAF (OR > 1, $P < .05$).

DAlPm and LAID are independent risk factors of moderate to severe MR in the patients with NVAF. NVAF can change the structure and function of mitral valve, which leads to MR.

Abbreviations: A2D = 2-dimensional area, AF = atrial fibrillation, C3D = 3-dimensional circumference, DAlPm = anterolateral-to-posteromedial diameter, DAP = anterior-to-posterior diameter, 2D-TTE = 2-dimensional transthoracic echocardiography, H = height, LAID = left atrial internal diameter, LVD = left ventricular diameter, LVEF = left ventricular ejection fraction, MR = mitral regurgitation, MVQ = mitral valve quantification, θNPA = nonplanar angle, NVAF = nonvalvular atrial fibrillation, PaAF = paroxysmal atrial fibrillation, PeAF = persistent atrial fibrillation, RT-3D-TEE = real-time 3-dimensional transoesophageal echocardiography, SR = sinus rhythm.

Keywords: atrial fibrillation, mitral valve, real-time 3-dimensional echocardiography

1. Introduction

Multiple factors, especially atrial fibrillation (AF) duration, affect the left atrial internal diameter (LAID) in the patients with nonvalvular AF (NVAF). The LAID changes are related to the occurrence and development of AF.[1,2] Mitral regurgitation (MR) is significantly correlated with LAID in the patients with AF. An increase in LAID may result in abnormalities of the mitral apparatus. MR is mainly caused by annulus dilation and abnormal leaflet configuration, and these changes can affect closure force balance and induce leaflet closure malfunctions. In this study, 65 patients with NVAF were served as research subjects.

Conventional M-mode echocardiography and 2-dimensional transthoracic echocardiography (2D-TTE) are important tools because they can be used to diagnose mitral valve diseases and provide a basis for anatomical and pathological structures. 2D-TTE is convenient, cheap, noninvasive, and highly reproducible. Color Doppler flow imaging is necessary to evaluate complex MR structures, but it cannot display the anatomy and corresponding relationship of the mitral valve. Real-time 3-dimensional transesophageal echocardiography (RT-3D-TEE) can easily show the structures of mitral valve, which conventional M-mode echocardiography and 2D-TTE are not able to display. With rapid advancements in ultrasound and software technology, RT-3D-TEE is greatly improved. RT-3D-TEE may be used to diagnose and analyze the specific geometries and pathology of mitral valve diseases by high-resolution images. RT-3D-TEE can show 3D image of the mitral valve on an "en-face" view from the left atrium (LA) with the aortic valve in the 12 O'clock position.

Editor: Wilhelm Mistiaen.

DH and CC contributed equally to this study.

The present study was supported by the National Natural Science Foundation of China (no. 81401419), the program of advanced study to go abroad in Henan provincial health system (no. 2016047), and the medical science and technology project of Henan province (no. 201602173).

The authors have no conflicts of interest to disclose.

Department of Cardiovascular Ultrasound, Henan Provincial People's Hospital/People's Hospital of Zhengzhou University, Zhengzhou, Henan, China.

** Correspondence: Lin Liu, Department of Cardiovascular Ultrasound, Henan Provincial People's Hospital/People's Hospital of Zhengzhou University, No. 7, Weiwu Road, Zhengzhou 450003, China (e-mail: liulin_819@126.com).*

Copyright © 2018 the Author(s). Published by Wolters Kluwer Health, Inc. This is an open access article distributed under the terms of the Creative Commons Attribution-Non Commercial-No Derivatives License 4.0 (CCBY-NC-ND), where it is permissible to download and share the work provided it is properly cited. The work cannot be changed in any way or used commercially without permission from the journal.

Medicine (2018) 97:33(e11643)

Received: 24 February 2018 / Accepted: 29 June 2018

http://dx.doi.org/10.1097/MD.0000000000011643

The QLAB mitral valve quantification (MVQ) software provides detailed anatomical structures of mitral valve which is conducive to online or offline quantitative measurements of mitral annulus and leaflet.[3,4]

This study aimed to explore the effects of NVAF on the structure and function of mitral valves and analyze independent risk factors of moderate to severe MR in the patients with NVAF by quantitative measurement of mitral annulus and leaflets using RT-3D-TEE, illustrating the mechanism of moderate to severe MR.

2. Methods

All study methods were approved by the Ethics Committee of Henan Provincial People's Hospital/People's Hospital of Zhengzhou University. All the subjects enrolled into the study gave written informed consent to participate.

2.1. Subjects

A total of 65 NVAF patients received radiofrequency ablation therapy in our hospital from July 2014 to August 2016. According to the 2014 AHA/ACC/HRS guidelines for the management of patients with AF,[5] the 65 patients were divided into 2 groups: paroxysmal AF group (PaAF group) and persistent AF group (PeAF group). Other 30 subjects with sinus rhythm (SR) were enrolled in SR group.

Moreover, according to the degree of MR,[6] the 65 NVAF patients were again divided into 2 groups: no or mild MR group and moderate to severe MR group. All patients underwent 2D-TTE and RT-3D-TEE.

After admission, all patients were diagnosed with PaAF or PeAF based on ECG and/or Holter monitoring. Exclusion criteria were rheumatic heart disease; mitral valve prolapse; congenital heart disease; prosthetic heart valves replacement; esophageal varices; esophageal neoplasms; and acute or chronic infective diseases.

2.2. 2-Dimensional transthoracic echocardiography

An iE33 ultrasound system (Philips Medical Systems, Andover, MA) with 1 to 5 MHz X5-1 probe was used in 2D-TTE. The patient lied in the left-side supine position. 2D-TTE was applied to measure LAID, left ventricular diameter (LVD), and left ventricular ejection fraction (LVEF) in the parasternal left ventricular long-axis view. To determine MR, color Doppler flow imaging of 3 consecutive cardiac cycles on both apical 4-chamber view and apical 2-chamber view was obtained, and their average values were calculated.

2.3. Real-time 3-dimensional transesophageal echocardiography

RT-3D images were obtained through a mid-esophageal view using a Philips iE33 (Philips Medical Systems, Andover, MA) ultrasound system equipped with a multiplane transesophageal X7-2t matrix array transducer.

Image acquisition: The mitral valve was imaged in the mid-esophageal 5-chamber views at 0°. The 3D-zoom imaging modality was selected to acquire the RT-3D images of the whole mitral valve, including the annulus, leaflets, and aortic valve. The image was rotated to resemble the surgical orientation, with the aorta at 12 O'clock (Fig. 1). RT-3D datasets were acquired several times to ensure optimal image quality without stitching artifacts. 3D-zoom images were obtained over 4 cardiac cycles at a frame rate of 10 to 30 frames per second.

Image analysis: All RT-3D echocardiographic data were analyzed offline using MVQ software, which is a part of QLAB suite (Philips Medical Systems). According to the electrocardiogram, the early and late systolic images were selected for the analysis. After the RT-3D data set was properly oriented, the software automatically displayed 4 quadrants: two 2D orthogonal-cut long-axis images of the mitral annulus, a mitral valve en-face image and a panel with the rendered 3D data. In this visualization, the operator can separately optimize the position of each of the 3 cut planes to identify the structures of mitral valve better. The image was oriented by adjusting the rotation of image data in the orthogonal planes to ensure that the mitral valve was bisected by the 2 long-axis planes, and the short-axis plane was parallel to the plane of the valve. The 4 major annulus reference points (anterolateral, posteromedial, anterior, and posterior) were initially tagged on the appropriate planes. The aortic root was manually labeled at the insertion of the

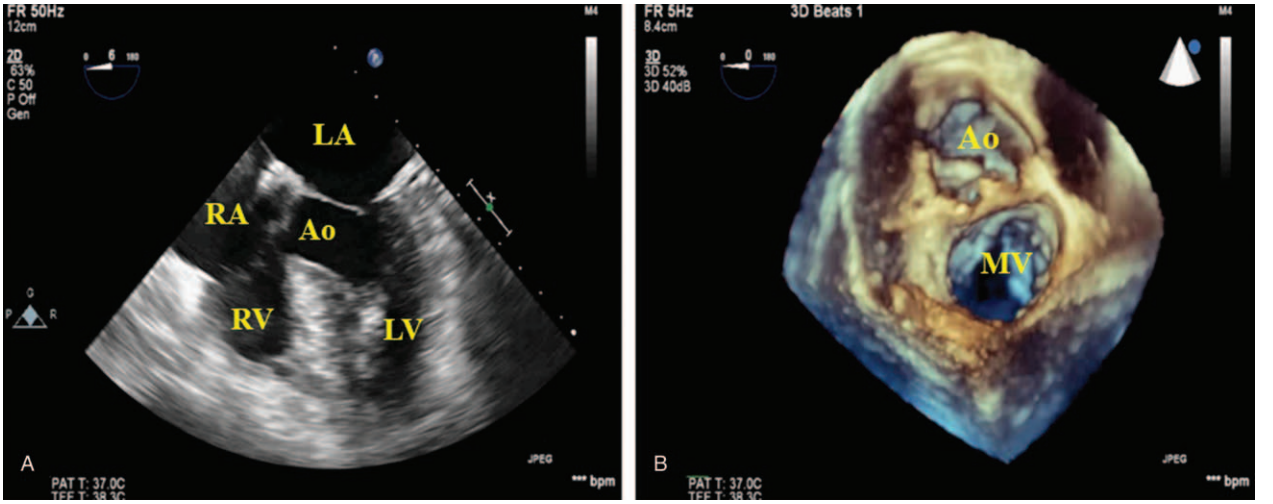

Figure 1. Image acquisition. A, Mitral valve in the midesophageal 5-chamber view. B, Mitral valve in 3D en-face view. Ao = aorta, LA = left atrial, LV = left ventricle, RA = right atrial, RV = right ventricle.

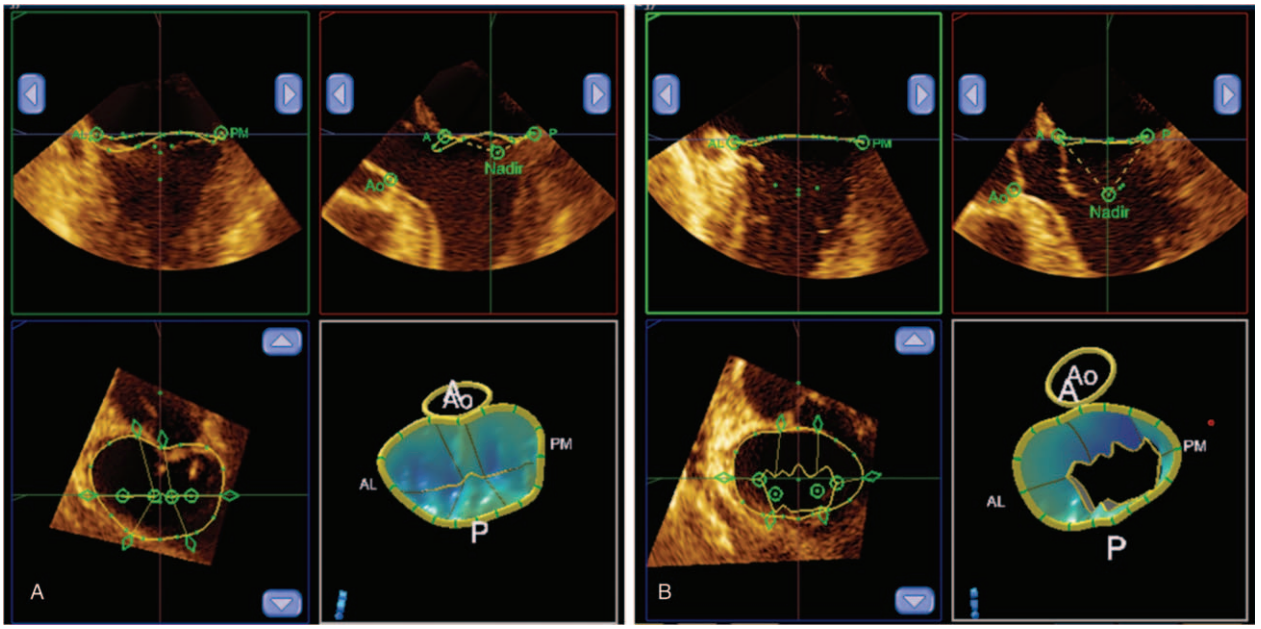

Figure 2. Image analyses, placing annular points and tracing leaflets. A, Mitral valve in end-systole phase. B, Mitral valve in early-diastolic phase. A = anterior, AL = anterolateral, Ao = aorta, P = posterior, PM = posteromedial.

posterior cusp into the sinus of Valsalva. The 3D annulus shape of the mitral valve obtained from these initial reference points was further initialized by placing a couple of annular points in 6 additional rotational cross-sections of the volumetric data set. As a result, 16 points were selected to define the mitral valve annulus. After the annular points were positioned, the leaflet profile was traced and the coaptation points were marked on multiple cut planes orthogonal to the anterolateral-posteromedial direction. The mitral valve was then segmented to map the leaflet contour and coaptation by manually tracing the leaflets in multiple parallel long-axis planes spanning the valve from commissure to commissure (6 trace points per centimeter) (Fig. 2). We could acquire 3D patterns of the mitral annulus and mitral valve leaflets after the operation was completed (Figs. 3 and 4), and then "report" was selected to generate the mitral valve–related parameters.

Several parameters were calculated from this model including mitral annulus parameters including anterolateral-to-posteromedial diameter (DAlPm), anterior-to-posterior diameter (DAP), height (H), 3-dimensional circumference (C3D), and 2-dimensional area (A2D) and mitral valve leaflet parameters including nonplanar angle (θNPA) of leaflets, mitral leaflet surface area in early diastolic phase, mitral leaflet surface area in late systolic phase, mitral valve coaptation area, and mitral valve coaptation index. Some parameters were calculated by the following formulas: mitral valve coaptation area = mitral leaflet surface area in early diastolic phase − mitral leaflet surface area in late systolic phase; the index of mitral valve coaptation (%) = (mitral valve coaptation area/mitral leaflet surface area in early diastolic phase) × 100%.

2.4. Statistical analysis

Data were statistically analyzed using SPSS 18.0 for Windows (IBM, Armonk, NY). Continuous data were expressed as mean ± SD and categorical variables were presented as absolute numbers or percentages. The continuous variables with normal distribution were analyzed using Kolmogorov-Smirnov test. Differences in measurement data were compared using *t* test. The mean values were compared by single-factor variance analysis among the 3 groups, and all pairwise comparisons were performed using LSD method. Numeration data were compared using χ^2 test. Inter-and intraobserver variabilities were assessed by Bland-Altman analysis. Differences were considered statistically significant at $P < .05$.

3. Results

3.1. Comparisons among different cardiac rhythm groups

PaAF group contained 35 patients including 17 men and 18 women with a mean age of 55.26 ± 4.80 years, PeAF group contained 30 patients including 20 men and 10 women with a mean age of 58.53 ± 4.50 years, and SR group contained 30 subjects including 14 men and 16 women with a mean age of 55.60 ± 3.96 years. PaAF group included 26 patients with no or mild MR and 9 patients with moderate to severe MR, and PeAF group included 18 patients with no or mild MR and 12 patients with moderate to severe MR. There were no significant differences in LVD, LVEF, sex, body mass index, hypertension, diabetes, thyroid diseases, smoking history, and drinking history among the 3 groups (all $P > .05$). Age, coronary heart disease, stroke, and LAID showed significant differences among the 3 groups (all $P < .05$, Table 1).

DAlPm, DAP, C3D, A2D, and mitral leaflet surface area in late systolic phase and mitral valve coaptation index were significantly different among the 3 groups (all $P < .05$). DAlPm and C3D were significantly greater, but mitral valve coaptation index was significantly lower in the PaAF group than in the SR group (all $P < .05$). DAlPm, DAP, C3D, A2D, and mitral leaflet surface area in the late systolic phase were significantly greater, but the mitral valve coaptation index was significantly lower in the PeAF group than the SR group (all $P < .05$). The mitral valve

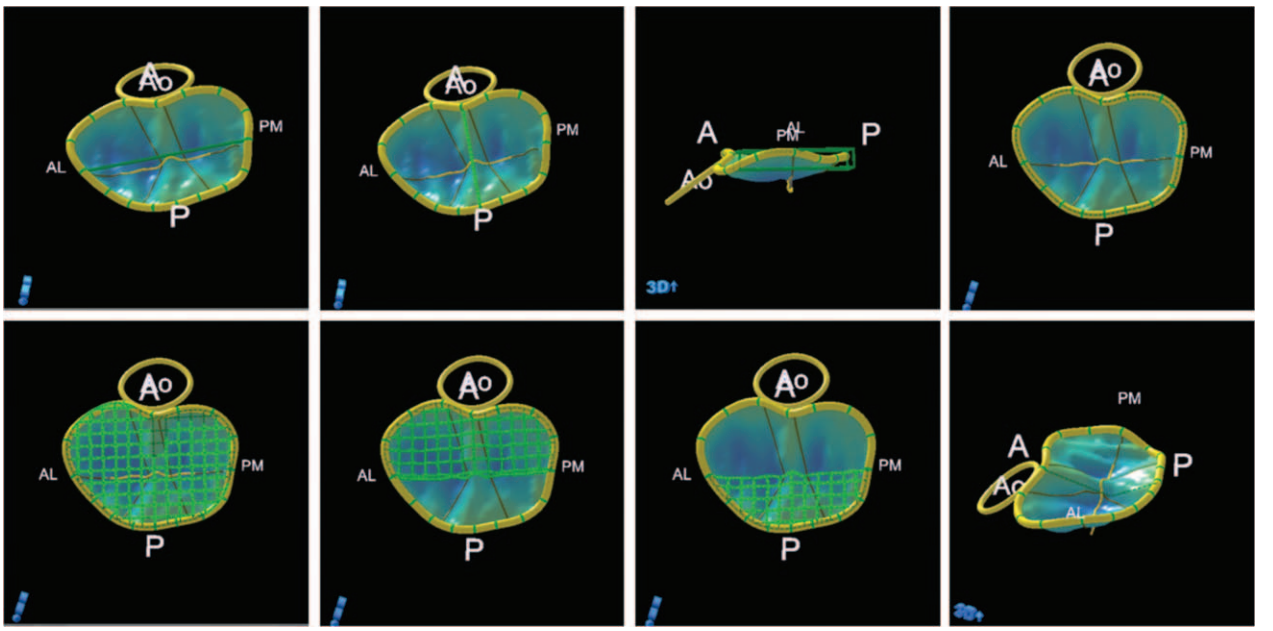

Figure 3. The 3D reconstruction of the mitral valve in late systolic phase, from which several parameters are automatically calculated.

parameters were not significantly different between PaAF and PeAF groups (all $P > .05$, Table 2).

3.2. Comparisons between different MR degrees

No or mild MR group contained 44 patients including 27 men and 17 women with a mean age of 55.41 ± 4.01 years, and moderate to severe MR group contained 21 patients including 10 men and 11 women with a mean age of 59.62 ± 5.47 years. Compared with no or mild MR group, LVD, LVEF, sex, body mass index, hypertension, diabetes, stroke, thyroid diseases, smoking history, and drinking history were not significantly different in the moderate to severe MR group (all $P > .05$). Age, coronary heart disease, and LAID were significantly different between the 2 groups (all $P < .05$, Table 3).

Compared with no or mild MR group, DAlPm, C3D, A2D, θNPA, and mitral leaflet surface area in the late systolic phase were significantly greater, whereas the mitral valve coaptation index was significantly lower in the moderate to severe MR group (all $P < .05$). Mitral valve coaptation area was not significantly different between the 2 groups ($P > .05$, Table 4)

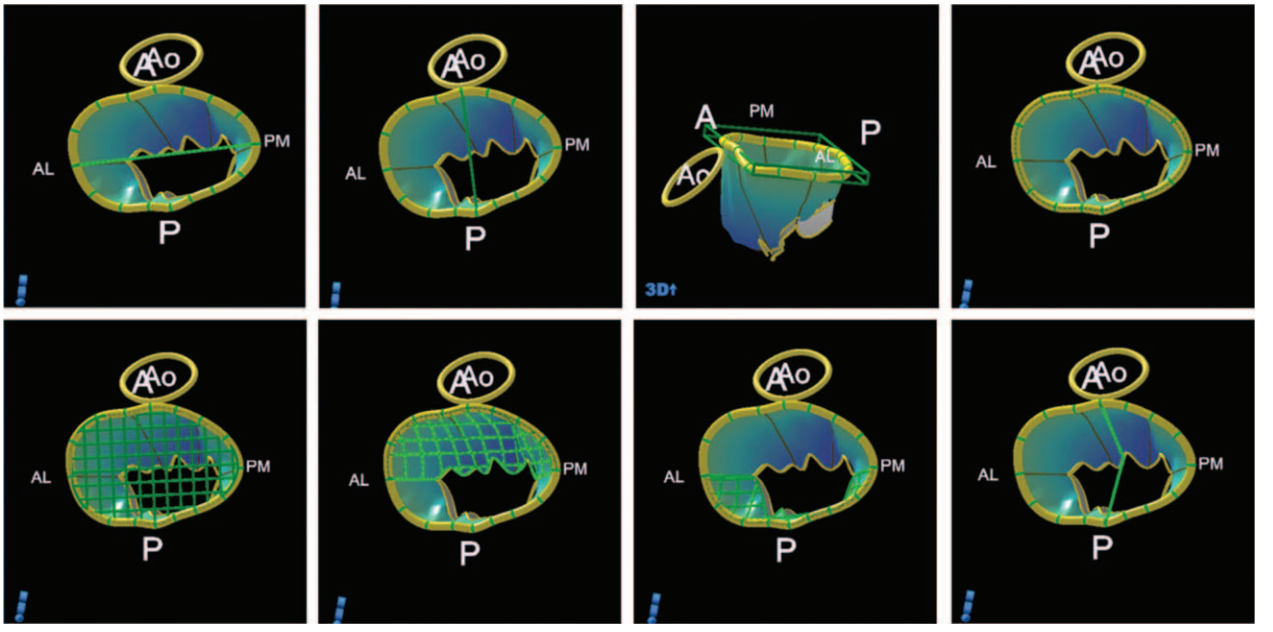

Figure 4. The 3D reconstruction of the mitral valve in early diastolic phase, from which several parameters are automatically calculated.

Table 1

Comparison of general data in different cardiac rhythm groups.

Variables	SR (n = 30)	PaAF (n = 35)	PeAF (n = 30)	P
Age, y	55.60 ± 3.96	55.26 ± 4.80	58.53 ± 4.50*	.008
Sex (female)	16 (53.3%)	18 (51.4%)	10 (33.3%)	.224
Body mass index, kg/m^2	22.59 ± 1.42	22.87 ± 1.76	23.45 ± 1.49	.102
LVD, mm	48.93 ± 2.56	49.83 ± 3.38	48.33 ± 2.91	.133
LVEF, %	59.47 ± 2.81	59.20 ± 2.39	59.40 ± 2.25	.903
LAID, mm	38.14 ± 4.32	43.20 ± 4.99*	45.46 ± 5.17*	.000
Hypertension	9 (30.3%)	11 (31.4%)	6 (20.0%)	.545
Coronary heart disease	7 (23.3%)	4 (11.4%)*	13 (43.3%)*	.012
Diabetes	4 (13.3%)	6 (17.1%)	8 (26.7%)	.396
Stroke	2 (6.7%)	5 (14.3%)*	9 (30.0%)*	.048
Thyroid diseases	1 (3.3%)	4 (11.4%)	2 (7.4%)	.453
Smoking history	7 (23.3%)	9 (25.7%)	10 (33.3%)	.660
Drinking history	7 (23.3%)	8 (22.9%)	7 (23.3%)	.999

LAID = left atrial internal diameter, LVD = left ventricular diameter, LVEF = left ventricular ejection fraction, PaAF = paroxysmal atrial fibrillation, PeAF = persistent atrial fibrillation, SR = sinus rhythm.
* $P < .05$ as compared with SR group.

3.3. Independent risk factors of moderate to severe MR in NVAF patients

Univariate analysis revealed that age, coronary heart disease, LAID, DAlPm, C3D, A2D, θNPA, mitral leaflet surface area in the late systolic phase, and mitral valve coaptation index were the risk factors of moderate to severe MR in NVAF patients ($P < .05$). Multivariate analysis indicated that DAlPm and LAID were the independent risk factors of moderate to severe MR in NVAF patients (OR > 1, $P < .05$, Table 5).

Table 2

Comparison of mitral valve parameters in different cardiac rhythm groups (mean ± SD).

Variables	SR (n = 30)	PaAF (n = 35)	PeAF (n = 30)	P
DAlPm, mm	33.54 ± 2.64	34.97 ± 2.63*	35.38 ± 2.15*	.013
DAP, mm	24.86 ± 2.97	25.95 ± 2.80	27.07 ± 3.56*	.026
H, mm	3.48 ± 0.71	3.46 ± 0.62	3.28 ± 0.78	.456
C3D, mm	102.26 ± 11.01	114.56 ± 13.79*	117.10 ± 14.46*	<.001
A2D, mm^2	765.21 ± 125.52	823.08 ± 153.78	897.43 ± 179.89*	.005
θNPA, °	117.96 ± 14.09	119.47 ± 12.73	123.57 ± 11.42	.216
Mitral leaflet surface area in late systolic phase, mm^2	814.77 ± 113.66	867.24 ± 112.65	920.04 ± 118.49*	.003
Mitral leaflet surface area in early diastolic phase, mm^2	1169.02 ± 153.84	1187.95 ± 136.72	1229.00 ± 134.71	.249
Mitral valve coaptation area, mm^2	349.58 ± 91.84	320.71 ± 94.08	308.96 ± 70.07	.177
Mitral valve coaptation index, %	29.91 ± 6.01	26.84 ± 6.51*	25.13 ± 4.79*	.008

A2D = 2-dimensional area, C3D = 3-dimensional circumference, DAlPm = anterolateral-to-posteromedial diameter, DAP = anterior-to-posterior diameter, H = height, θNPA = non-planarity angle, PaAF = paroxysmal atrial fibrillation, PeAF = persistent atrial fibrillation, SR = sinus rhythm.
* $P < .05$ as compared with SR group.

Table 3

Comparison of the general data between different mitral regurgitation degrees.

Variables	No or mild MR (n = 44)	Moderate or severe MR (n = 21)	P
Age, y	55.41 ± 4.01	59.62 ± 5.47*	.001
Sex (female)	17 (38.6%)	11 (52.4%)	.295
Body mass index, kg/m^2	23.33 ± 1.63	22.73 ± 1.66	.172
LVD, mm	48.77 ± 2.95	49.90 ± 3.73	.189
LVEF, %	59.27 ± 2.2	59.33 ± 2.4	.922
LAID, mm	43.05 ± 4.45	46.75 ± 5.74*	.006
Hypertension	12 (27.3%)	5 (23.8%)	.766
Coronary heart disease	8 (18.2%)	9 (42.9%)*	.034
Diabetes	11 (25.0%)	3 (14.3%)	.520
Stroke	9 (20.5%)	5 (23.8%)	.757
Thyroid diseases	5 (11.4%)	1 (4.8%)	.655
Smoking history	11 (25.0%)	8 (38.1%)	.278
Drinking history	9 (20.5%)	6 (28.6%)	.468

LAID = left atrial internal diameter, LVD = left ventricular diameter, LVEF = left ventricular ejection fraction, MR = mitral regurgitation,.
* $P < .05$ as compared with no or mild MR group.

3.4. Inter- and intraobserver variability

The inter- and intraobserver agreements of the assessment with Bland-Altman analysis of DAlPm, DAP, H, C3D, A2D, θNPA, mitral valve coaptation area, and mitral valve coaptation index with RT-3D-TEE slightly differed and exhibited fair limits of agreement (Figs. 5 and 6).

4. Discussion

AF has severe symptoms and may lead to low quality of life, especially MR.[7,8] RT-3D-TEE has advantages in accurate diagnosis of MR as compared with conventional 2D-TTE. In NVAF patients, dynamic pattern of the annulus is different from that of normal individuals. RT-3D-TEE data sets can be used to

Table 4

Comparison of mitral valve parameters between different mitral regurgitation degrees (mean ± SD).

Variables	No or mild MR (n = 44)	Moderate or severe MR (n = 21)	P
DAlPm, mm	34.08 ± 1.90	37.40 ± 1.73*	<.001
DAP, mm	26.09 ± 3.00	27.25 ± 3.54	.176
H, mm	3.47 ± 0.67	3.19 ± 0.74	.128
C3D, mm	113.04 ± 13.76	121.37 ± 13.24*	.024
A2D, mm^2	825.03 ± 159.10	925.21 ± 173.30*	.024
θNPA, °	119.25 ± 11.37	125.80 ± 13.04*	.042
Mitral leaflet surface area in late systolic phase, mm^2	863.73 ± 109.71	950.01 ± 114.06*	.005
Mitral leaflet surface area in early diastolic phase, mm^2	1192.59 ± 137.59	1236.88 ± 131.73	.223
Mitral valve coaptation area, mm^2	328.86 ± 87.67	286.86 ± 67.08	.057
Mitral valve coaptation index, %	27.44 ± 5.83	23.15 ± 4.65*	.005

A2D = 2-dimensional area, C3D = 3-dimensional circumference, DAlPm = anterolateral-to-posteromedial diameter, DAP = anterior-to-posterior diameter, H = height, MR = mitral regurgitation, θNPA = non-planarity angle.
* $P < .05$ as compared with no or mild MR group.

Table 5

The independent risk factors of moderate to severe mitral regurgitation in nonvalvular atrial fibrillation patients.

Variables	B	SE	Wals	Sig.	Exp (B)	95% CI
DAlPm	1.049	0.274	14.685	<0.001	2.855	1.669–4.882
LAID	0.172	0.086	4.007	0.045	1.188	1.004–1.405
Constant	−46.028	11.641	15.634	<0.001	<0.001	

CI = confidence interval, DAlPm = anterolateral-to-posteromedial diameter, LAID = left atrial internal diameter.

measure different parameters that describe the abnormal geometry of the mitral annulus and valve leaflet to elucidate the pathogenesis of NVAF. This study demonstrates that NVAF can change the structure and function of mitral valve and lead to MR. RT-3D-TEE can analyze the change of 3D structure of mitral valve in the patients with NVAF and illustrate the mechanism of moderate to severe MR.

Atrial remodeling includes atrial electrical and structural remodeling.[9–11] LA enlargement leads to neurohormonal activation, and atrial stretch and fibrosis, which can facilitate the initiation and maintenance of AF. Atrial fibrosis may promote atrial electrical remodeling and maintain AF.[12–14] The findings of this study suggest that LAID is greater in the PaAF and PeAF groups ($P < .05$) than in the SR group. The types of AF and the lasting time of AF are associated with LAID. Long AF duration increases the degree of atrial expansion. LAID is, however, not significantly different between the PaAF and PeAF groups ($P > .05$). LAID is possibly related to course of disease, which needs to be further confirmed.

The mitral annulus, which is oval and saddle-shaped, constitutes the anatomical junction between the LV and LA and serves as the insertion site for leaflet tissues. The highest points of the saddle of the annulus are located anteriorly and posteriorly, and the lowest points are located at the level of the commissures. The mitral valve has a complex 3D structure and its morphology is related to its function. The anterior aspect of the annulus is less and prone to dilation, because it is attached to the fibrous trigones. The posterior annulus receives some muscular fibers from the proximal aspect of the posterior leaflet, which may affect annular flexibility. Hence, the posterior annulus is susceptible to traction in pathologic conditions.

An enlarged LA, particularly caused by AF, is significantly associated with mitral annular dilation through the mechanism of atrial remodeling.[15] In this study, DAlPm, DAP, C3D, and A2D were significantly different among the different cardiac rhythm groups ($P < .05$). Compared with those of the SR group, DAlPm and C3D were greater in PaAF group ($P < .05$), but DAP was not significantly different; moreover, DAlPm, DAP, C3D, and A2D were greater in the PeAF group ($P < .05$). The increased DAlPm in PaAF patients suggests that annular dilatation occurs in the anterolateral to posteromedial directions, without significantly changed DAP. AF had less effect on H and θNPA, thereby explaining that the saddle-shaped mitral annulus maintained its initial H and nonplanar features in NVAF patients. When the θNPA was increased, the normal saddle-shaped mitral annulus was flattened and enlarged.

A good saddle-shaped mitral annulus is a basis for ensuring normal mitral valve function.[15,16] LA enlargement could increase the tension in the radial direction of the mitral annulus. The expansion and deformation of the mitral annulus lead to MR. Enlarged annular size would reduce the height of the annulus.[17] In this study, compared with no or mild MR group, DAlPm, C3D, A2D, θNPA, and LAID are greater in moderate to severe MR group ($P < .05$). Our results suggest that the structure and shape of mitral annulus are abnormal in moderate to severe MR, which is associated with MR. A smaller θNPA can guarantee the maintenance of nonplanar geometry of mitral annulus.

The anterior leaflet includes smooth and coarse regions, whereas the posterior leaflet includes basal, smooth, and coarse regions. The coarse region is the effective contact region between anterior and posterior leaflets and mainly ensures normal mitral valve function.[18]

The fibrous tissue of the posterior annulus, to which the posterior leaflet attaches, is weak. When LA is enlarged in

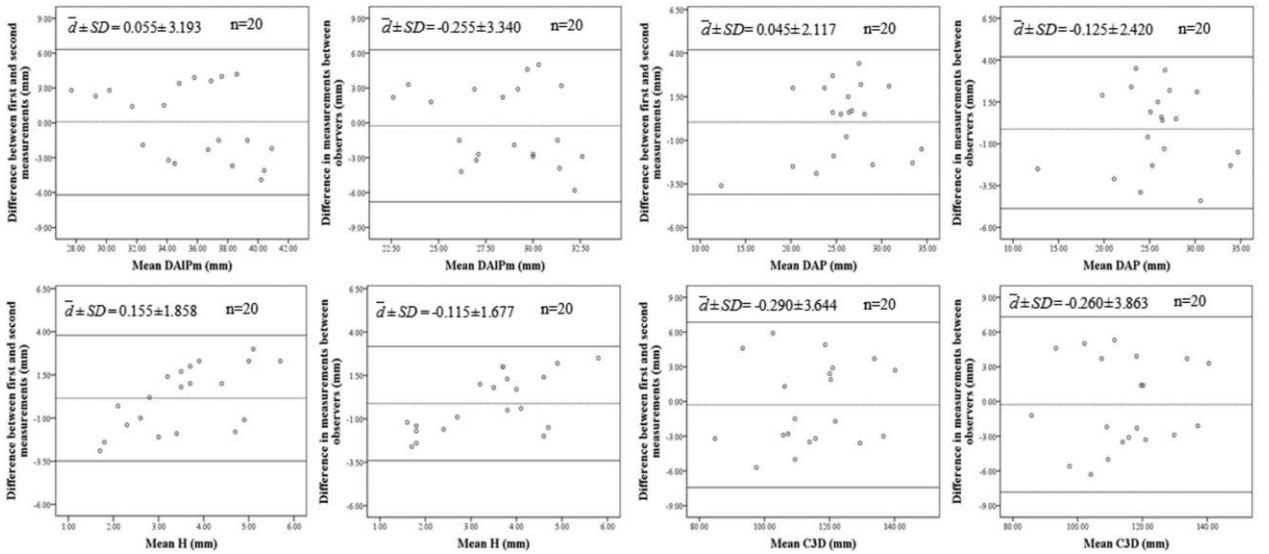

Figure 5. Bland-Altman plots showing interobserver and intraobserver differences and limits of agreement of DAlPm, DAP, H, and C3D measured by RT-3D-TEE. The solid line represents the mean difference between the measurements analyzed by 1 observer or by 2 observers, and the dashed lines represent the 95% confidence interval for agreement. $\bar{d} \pm$ SD: mean ± standard deviation.

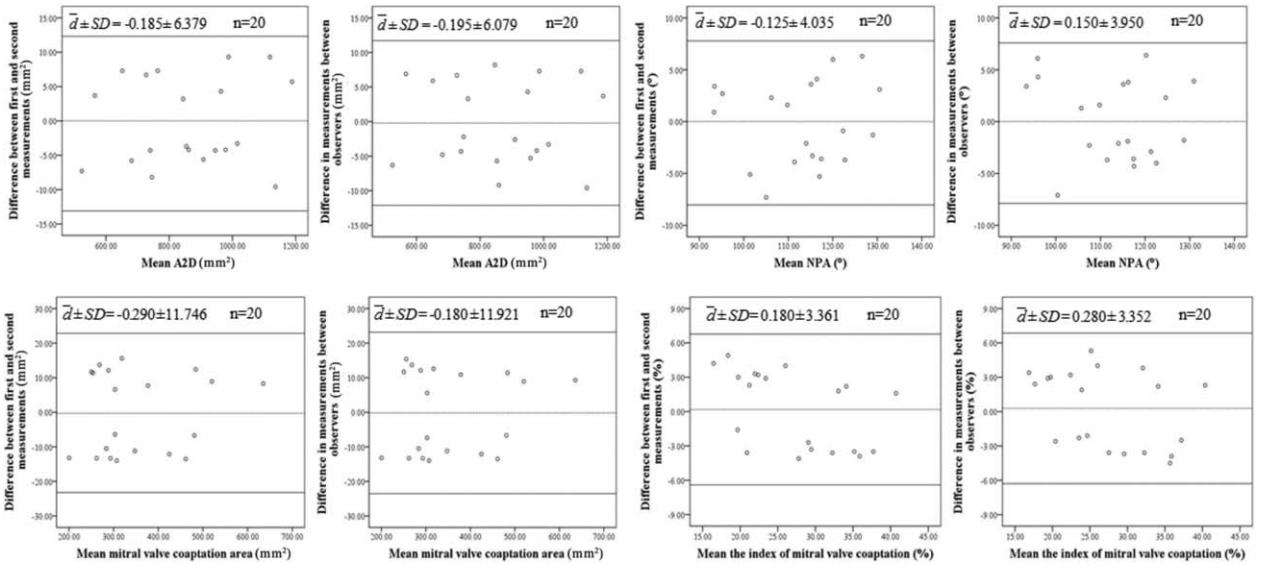

Figure 6. Bland-Altman plots showing interobserver and intraobserver differences and limits of agreement of A2D, θNPA, mitral valve coaptation area, and mitral valve coaptation index measured by RT-3D-TEE. The solid line represents the mean difference between the measurements analyzed by 1 observer or by 2 observers, and the dashed lines represent the 95% confidence interval for agreement. $\bar{d} \pm$ SD: mean ± standard deviation.

patients with AF, the posterior annulus is tensed, thereby leading to annulus enlargement. And, annular dynamic motion affects leaflet coaptation. Substantial leaflet surplus may compensate the enlarged mitral orifice size within a certain extent. The coaptation of mitral leaflet may be improved by that the size of mitral annulus is reduced during early systole and the saddle shape of mitral annulus becomes deep.[19,20] More than a certain extent, however, the leaflets can no longer overcome the increased annular dimensions, leading to mitral insufficiency.

This study indicated no significant difference in mitral leaflet surface area in early diastolic phases among the different cardiac rhythm groups ($P > .05$). With mitral annulus expansion, mitral leaflet areas in early diastolic phase did not increase in AF patients. Compared with the SR group, the mitral leaflet surface area in late systolic phase was larger in the PeAF group ($P < .05$), indicating that the effective contact region between anterior and posterior leaflets was reduced, leading to MR. Moreover, compared with the SR group, the mitral valve coaptation area was not significantly different (all $P > .05$); but, the mitral valve coaptation index was smaller in PaAF and PeAF groups (all $P < .05$). These results were different from previous studies,[21] which may be related to different patient's body surface areas, heart sizes, and so on. Therefore, the parameters of mitral valve coaptation index are only used to correct the coaptation area and evaluate the mitral valve precisely. Compared with the no or mild MR group, the mitral valve coaptation index was smaller in the moderate to severe MR group ($P < .05$), confirming that mitral valve coaptation index can objectively evaluate mitral valve function.

The prevalence rate of coronary heart disease in the moderate to severe MR group was significantly higher than that in the no or mild MR group ($P < .05$). This finding indicated that coronary heart disease is a potential risk factor of mitral valve insufficiency in NVAF patients. The univariate predictors of moderate to severe MR were coronary heart disease, LAID, DAlPm, C3D, A2D, θNPA, mitral leaflet surface area in late systolic phase, and mitral valve coaptation index. These factors were subsequently incorporated into a forward stepwise multivariate model. After analysis, DAlPm and LAID were the predictors of moderate to severe MR in NVAF patients. Moderate to severe MR in NVAF patients was strongly associated with DAlPm and LAID. Moreover, the morphology, structure, and function of LA are involved in the mechanism of moderate to severe MR.

4.1. Limitation

This study had several limitations. First, mitral valve morphology was evaluated immediately when the patient was under anesthesia instead of a physiologic state. As such, biases in measurements could be potentially introduced. Second, annular control points and leaflet profiles were traced manually, so the whole analysis process was time consuming. Third, the disk summation algorithm should be used to measure LA volumes to avoid the influences of image positioning and operator measurement errors. Fourth, RT-3D-TEE is easily affected by patient's posture, obesity, thoracic gas, and other factors. Finally, the study population was small. Hence, it is necessary to further confirm our results.

5. Conclusion

Based on RT-3D-TEE results of MR, NVAF can change the structure and function of mitral valve, which is associated with MR.

Author contributions

Conceptualization: Lin Liu.
Data curation: Cun-ying Cui, Lian-zhong Zhang.
Formal analysis: Juan Zhang.
Investigation: Yuan-yuan Liu.
Methodology: Yun-yun Qin.
Writing – original draft: Dan-qing Huang.
Writing – review and editing: Lin Liu.

References

[1] Xu J, Xu X, Si L, et al. Intracellular lactate signaling cascade in atrial remodeling of mitral valvular patients with atrial fibrillation. J Cardiothorac Surg 2013;8:34.

[2] Kannel WB, Wolf PA, Benjamin EJ, et al. Prevalence, incidence, prognosis, and predisposing conditions for atrial fibrillation: population-based estimates. Am J Cardiol 1998;82:2N–9N.

[3] Hyodo E, Iwata S, Tugcu A, et al. Direct measurement of multiple vena contracta areas for assessing the severity of mitral regurgitation using 3D TEE. JACC Cardiovasc Imaging 2012;5:669–76.

[4] Caiani EG, Fusini L, Veronesi F, et al. Quantification of mitral annulus dynamic morphology in patients with mitral valve prolapse undergoing repair and annuloplasty during a 6-month follow-up. Eur J Echocardiogr 2011;12:375–83.

[5] January CT, Wann LS, Alpert JS, et al. ACC/AHA Task Force Members2014 AHA/ACC/HRS guideline for the management of patients with atrial fibrillation: executive summary: a report of the American College of Cardiology/American Heart Association Task Force on practice guidelines and the Heart Rhythm Society. Circulation 2014;130:2071–104.

[6] Helmcke F, Nanda NC, Hsiung MC, et al. Color Doppler assessment of mitral regurgitation with orthogonal planes. Circulation 1987;75: 175–83.

[7] Messika-Zeitoun D, Bellamy M, Avierinos JF, et al. Left atrial remodelling in mitral regurgitation—methodologic approach, physiological determinants, and outcome implications: a prospective quantitative Doppler-echocardiographic and electron beam-computed tomographic study. Eur Heart J 2007;28:1773–81.

[8] Gertz ZM, Raina A, Saghy L, et al. Evidence of atrial functional mitral regurgitation due to atrial fibrillation: reversal with arrhythmia control. J Am Coll Cardiol 2011;58:1474–81.

[9] Fuster V, Ryden LE, Cannom DS, et al. Task Force on Prectice Guidelines, American College of Cardiology/American Heart Association, Committee for Practice Guidelines, European Society of Cardiology, European Heart Rhythm Association, Heart Rhythm Society.ACC/AHA/ESC 2006 guidelines for the management of patients with atrial fibrillation-executive summary: a report of the American College of Cardiology/American Heart Association Task Force on Practice Guidelines and the European Society of Cardiology Committee for Practice Guidelines (Writing Committee to Revise the 2001 Guidelines for the Management of Patients with Atrial Fibrillation). Eur Heart J 2006;27: 1979–2030.

[10] McDowell KS, Vadakkumpadan F, Blake R, et al. Mechanistic inquiry into the role of tissue remodeling in fibrotic lesions in human atrial fibrillation. Biophys J 2013;104:2764–73.

[11] Everett TT, Wilson EE, Verheule S, et al. Structural atrial remodeling alters the substrate and spatiotemporal organization of atrial fibrillation: a comparison in canine models of structural and electrical atrial remodeling. Am J Physiol Heart Circ Physiol 2006;291:H2911–23.

[12] Parkash R, Green MS, Kerr CR, et al. Canadian Registry of Atrial FibrillationThe association of left atrial size and occurrence of atrial fibrillation: a prospective cohort study from the Canadian Registry of Atrial Fibrillation. Am Heart J 2004;148:649–54.

[13] Erdei T, Denes M, Kardos A, et al. Could successful cryoballoon ablation of paroxysmal atrial fibrillation prevent progressive left atrial remodeling? Cardiovasc Ultrasound 2012;10:11.

[14] McManus DD, Xanthakis V, Sullivan L, et al. Longitudinal tracking of left atrial diameter over the adult life course: clinical correlates in the community. Circulation 2010;121:667–74.

[15] Veronesi F, Corsi C, Sugeng L, et al. Quantification of mitral apparatus dynamics in functional and ischemic mitral regurgitation using real-time 3-dimensional echocardiography. J Am Soc Echocardiogr 2008;21: 347–54.

[16] Watanabe N, Ogasawara Y, Yamaura Y, et al. Quantitation of mitral valve tenting in ischemic mitral regurgitation by transthoracic real-time three-dimensional echocardiography. J Am Coll Cardiol 2005;45: 763–9.

[17] Lee AP, Hsiung MC, Salgo IS, et al. Quantitative analysis of mitral valve morphology in mitral valve prolapse with real-time 3-dimensional echocardiography: importance of annular saddle shape in the pathogenesis of mitral regurgitation. Circulation 2013;127:832–41.

[18] Cobey FC, Swaminathan M, Phillips-Bute B, et al. Quantitative assessment of mitral valve coaptation using three-dimensional transesophageal echocardiography. Ann Thorac Surg 2014;97: 1998–2004.

[19] Rausch MK, Bothe W, Kvitting JP, et al. Characterization of mitral valve annular dynamics in the beating heart. Ann Biomed Eng 2011;39: 1690–702.

[20] Daimon M, Saracino G, Fukuda S, et al. Dynamic change of mitral annular geometry and motion in ischemic mitral regurgitation assessed by a computerized 3D echo method. Echocardiography 2010;27:1069–77.

[21] Yamada R, Watanabe N, Kume T, et al. Quantitative measurement of mitral valve coaptation in functional mitral regurgitation: in vivo experimental study by real-time three-dimensional echocardiography. J Cardiol 2009;53:94–101.